Temperature Measurements of Falling Droplets

M. R. Wells

L. A. Melton

Department of Chemistry,
The University of Texas at Dallas,
Richardson, TX 75083

The temperature of 225-μm-dia decane droplets, which have fallen 100 mm through a hot quiescent, oxygen-free environment, has been measured using exciplex fluorescence thermometry. The droplets were doped with pyrene, and the relative intensities of pyrene monomer and excimer emissions were used to determine the droplet temperatures. The droplet temperature increases approximately 0.4°C per °C increase in the ambient temperature up to an ambient temperature of 200°C. Less than 10 percent evaporation was observed for the droplets at the highest ambient temperatures.

I Introduction

Vaporization in fuel sprays is a complex phenomenon involving heat and mass transfer in a dynamic mixture of droplets, fuel vapor, and ambient gas. Most workers in the field attempt to understand these processes in sprays by treating sprays as aggregates of individual drops, and therefore, understanding the processes that govern vaporization of individual fuel droplets becomes paramount. Many studies, both computational and empirical, of droplet vaporization have been performed, and reviews of the current understanding are available in the literature (Law, 1982; Sirignano, 1988; Faeth, 1983; Abramzon and Sirignano, 1988; Dwyer and Sanders, 1986; Aggarwal et al., 1984; Puri and Libby, 1988; Gogos and Ayyaswamy, 1988; Sirignano, 1983; Law and Sirignano, 1977; Prakash and Sirignano, 1978).

The vaporization of individual fuel droplets is generally studied photographically, a technique that yields only the droplet diameter (Puri and Libby, 1988; Aggarwal and Chen, 1989). A critical parameter in determining droplet evaporation rates is the temperature, specifically the surface temperature, of the droplets, and currently, few measurements of the temperature of vaporizing droplets are available. Charlesworth and Marshall (1959) measured the evaporation rates and temperatures of suspended water droplets by use of microthermocouples placed within the droplets. Trommelen and Crosby (1970), using a similar technique, measured evaporation rates and temperatures of suspended water droplets in various drying media. Abdul-Rahman (1969) measured the evaporation rates and temperature profiles of suspended water droplets by use of microthermocouples placed within the droplets. Hofmeister et al. (1989) measured surface temperatures of falling droplets of molten metals using two-color pyrometry.

Determination of the temperature of a droplet using thermocouples unavoidably perturbs both the droplet and the environment surrounding it and may alter the transfer of heat into or away from the droplet. In addition, suspended droplets are in physical contact with a support structure that may similarly make interpretation of the data uncertain. In this paper we describe the determination of the temperature of a decane droplet falling in a hot, relatively quiescent environment. The optical techniques described here can provide instantaneous, minimally perturbing measurement of even the surface temperatures of freely moving fuel droplets.

The technique used to measure the droplet surface temperature is exciplex fluorescence thermometry (EFT), which exploits the temperature-dependent fluorescence resulting from the reaction of an excited dopant molecule to form an exciplex, or excited-state complex (Murray and Melton, 1985). Room-temperature droplets were allowed to fall into an oven, and after falling 100 mm were intercepted by a laser beam that induced fluorescence of the dopant molecules. Analysis of the resulting fluorescence indicates that the temperature of the droplets increases aproximately 0.4°C per °C of increase in the ambient temperature as the ambient temperature is increased to 200°C.

II Exciplex Photophysics and Thermometry

The use of exciplexes as thermometers for bulk liquids and droplets has been discussed by Murray and Melton (1985), Melton et al. (1986), and Gossage and Melton (1987). More general reviews of the photophysics of fluorescence from exciplexes are available from Forster (1969) and Birks (1970). Recently, Stufflebeam (1989) has applied exciplex fluorescence thermometry to the determination of the temperature of bulk hydrocarbon liquids.

The photophysics of exciplex fluorescence thermometry is summarized in equation (1). A ground state molecule M (the monomer) may be excited by absorption of light to form the first excited singlet state M^*. M^* may react with an appropriately chosen ground state molecule G (which may be another M) to form an excited state complex E^* (exciplex), (excited state dimer or excimer if $G=M$). This reaction is shown by

$$M^* + G(M) \langle = = \rangle E^* \qquad (1)$$

E^* is bound with respect to M^* and G, but ground states M and G have little interaction; thus, fluorescence emission from E^* is red-shifted relative to that from M^*. The emission spec-

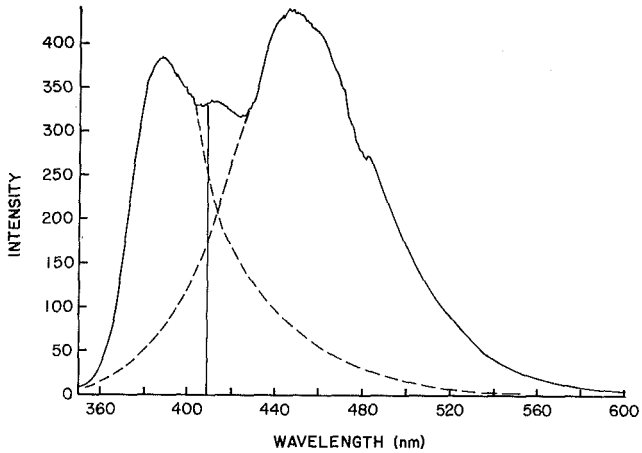

Fig. 1 Fluorescence spectrum of 5 mM pyrene in decane at 80°C, excitation wavelength 337 nm. Dashed lines are estimated extensions of monomer and excimer spectra, respectively. Vertical line at 408 nm is separation between monomer and excimer intensity integrals.

Contributed by the Heat Transfer Division for publication in the JOURNAL OF HEAT TRANSFER. Manuscript received by the Heat Transfer Division October 26, 1989; revision received March 21, 1990. Keywords: Flow Visualization, Measurement Techniques, Sprays/Droplets.

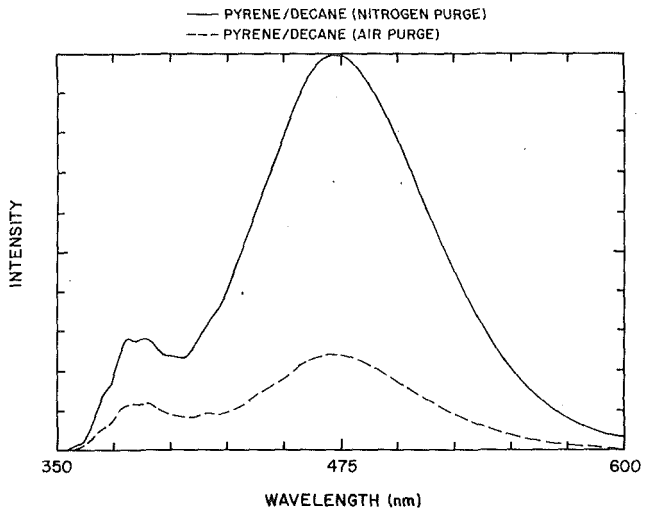

Fig. 2 Fluorescence spectra of 5-nM pyrene in decane, excitation wavelength 337 nm. Solid line is with nitrogen-purged solution; dashed line is with air-saturated solution.

trum may then exhibit two distinct emission bands, one from M^* and the other from E^*, as shown in Fig. 1. At sufficiently high temperatures, the forward and reverse rates of the reaction shown in equation (1) will be sufficiently fast that the reaction may be treated as a chemical equilibrium, whose position will depend upon the temperature and concentrations. Increasing the temperature will shift the equilibrium toward the monomer; thus, the amount of emission from E^* relative to that from M^* will decrease with increasing temperature. Increasing the concentration of G will shift the equilibrium toward E^*. The temperature-dependent ratio of the exciplex emission intensity (I_E) to the monomer emission intensity (I_M), at constant composition, can therefore be used as the basis for an optical thermometer.

The ratio I_E/I_M can be affected by factors other than temperature and dopant concentrations. Forster (1969) has demonstrated that dissolved molecular oxygen in the system will quench the fluorescence from both the monomer and excimer, the excimer exhibiting greater quenching than the monomer. Shown in Fig. 2 are spectra taken under both nitrogen-purged and air-saturated conditions for the 5.00×10^{-3} (5.00 mM) pyrene in decane solution used in the droplet studies. I_M and I_E are approximately 2 and 4 times greater, respectively, under oxygen-free conditions than under air-saturated conditions. Thus, oxygen-free conditions must be maintained during exciplex thermometry experiments, since the differential quenching of the fluorescence of the pyrene-doped droplets by the oxygen in air could easily result in erroneously high values of the temperature inferred for the droplets.

III Experimental

(A) Chemicals and Solutions. Reagent grade decane (99 + percent purity) was used to model a typical hydrocarbon fuel. It was purchased from Aldrich Chemical Company and used as received. Fluorescence measurements of the decane used indicated no detectable fluorescence. Pyrene was purchased from Aldrich Chemical Company and was sublimed (120°C, 1 torr) before use; unsublimed pyrene did not give reproducible results. A 5.00 mM solution of pyrene in decane was prepared and used both for droplet production and for calibration. Nitrogen gas (99.99 percent purity) was purchased from Big Three Inc. and used as received. The pyrene in decane solution was purged with nitrogen to remove dissolved oxygen in all experiments.

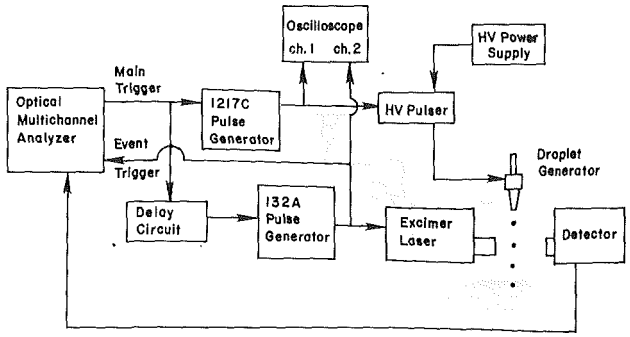

Fig 3 Block diagram of electronics

(B) Experimental Apparatus and Procedures. Droplets of a 5.00 mM solution of pyrene in decane were produced using a piezoelectric droplet generator of a design described generally by Shield et al. (1987). The piezoelectric transducer used in the construction of the droplet generator was purchased from E.B.L. Company (East Hartford, CT) and has dimensions of 11 mm × 9.5 mm o.d. × 4.5 mm i.d. The outside and inside surfaces of the transducer are nickel-plated for electrical contact, with the outer surface forming the positive pole. A jeweler's microtorch tip cut from a #3 Little Torch (Tescom Corp, Minneapolis, MN) was used as a nozzle. The microtorch tip has a sapphire insert with a 0.011-in. (approx. 280 μm) laser-drilled orifice. The torch tip was attached to the piezoelectric transducer with quick-setting epoxy. The droplet generator was supplied from a solution reservoir whose height could be adjusted to control the liquid head on the droplet generator. The pyrene in decane solution in the fluid reservoir was maintained under continuous nitrogen purge throughout all experiments. In addition, before each temperature run, enough solution was purged from the fluid system to ensure that only oxygen-free liquid was present in the lines.

A block diagram of the electronics used in the experiment is shown in Fig. 3. Fluorescence data collection, processing, and experimental control were performed by an EG & G PARC OMA III optical multichannel analyzer Model 1460-V consisting of an M1420 intensified photo diode array detector, a Model 1463 detector controller, an M1303 gated pulse interface, and a Jarrell-Ash Monospec 27 monochromator (150 g/mm ruling, dispersion 24 nm/mm). The detector was operated in a feed-back mode so that light integration did not commence until firing of the laser was detected. An output pulse (5 V TTL, 16 μs) from the OMA was amplified to approximately 25 V by a General Radio Model 1217-C pulse generator operated in the external trigger mode. The amplified pulse was sent to a custom-built high-voltage pulser powered by Tennelec Model TC 952 high-voltage power supply and was monitored by a Hitachi Model V-55B 50 MHz oscilloscope. The high-voltage output of the pulser, typically 900 V and 2 ms pulse width, was used to drive the droplet generator. The pulse originating from the OMA was also sent to a custom-built signal delay device (0-300 ms) and then amplified to 40 V (pulse width 2 ms) by an EH Research Model 132A pulse generator operated in the external trigger mode. This pulse was then sent to the Lumonics Model TE 861S pulsed excimer laser, which was operated as an N_2 laser (337 nm, 8 ns FWHM). The pulse energy was typically 1.5 mJ per pulse, as measured with a Scientech Power Energy Meter Model 36-2002 fitted with a Model 36-0001 disk calorimeter. The delayed pulse was also sent back to the OMA to initiate readout of the detector. For the droplet temperature measurements, typical laser pulse rates were 1 Hz.

The droplet generator/heated chamber assembly is shown in Fig. 4. The droplet generator was positioned on a water-cooled cold stage set 15 mm above a 150 mm long × 50 mm diameter cylindrical brass block. The nozzle tube of the droplet

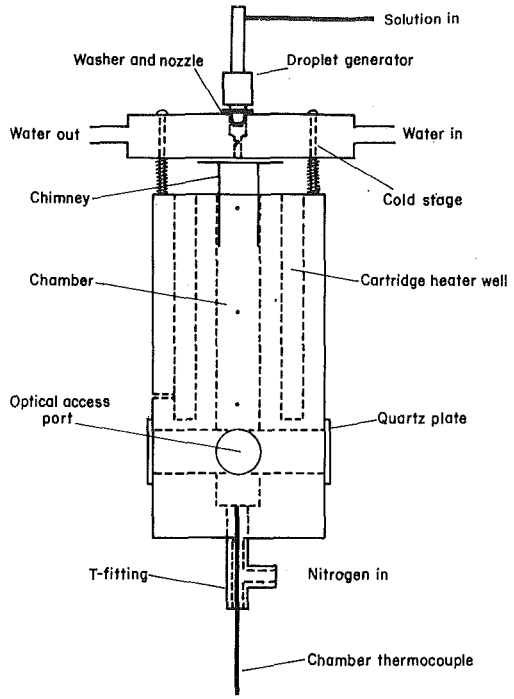

Fig. 4 Diagram of droplet generator/heated chamber assembly

generator was equipped with a snuggly fitting metal washer, which rested on the top of the cold stage. The washer provided good thermal contact between the cold stage and the nozzle tube and sealed the opening around the tube. In this manner, hot gases were prevented from streaming past the tube and heating it. Droplets exited the cold stage through a 1.3-mm orifice in its base. Below the cold stage, droplets entered a 150 mm × 16 mm square channel milled axially through the center of the brass block. A square-section chimney constructed of aluminum sheet (soft drink can, approx. 0.13 mm thick) was inserted into the top of the square channel in the block and was raised within 1 mm of the base of the cold stage. The chimney was lowered to allow photographic measurements of droplets immediately after they emerged from the base of the cold stage. For optical access, four circular ports (approx. 10 mm in. diameter) were positioned with their centers 85 mm from the top of the block. The port were covered with 2-mm-thick quartz windows to reduce convection-induced turbulence within the chamber due to air drawn in through the ports. Four cartridge heaters (each 150 W maximum at 240 V) were inserted into the brass block parallel to its axis and were supplied by a variable autotransformer. Heated nitrogen gas was admitted into the block from the bottom at flow rates from 140 to 180 ml/min, for linear flow velocities of 3.0 to 3.9 cm/s (corrected for thermal expansion within the heated chamber). The Reynolds number, based on the square chamber, for the nitrogen flowing through the chamber was calculated to be 28 at 20°C, and decreased to 13 to 250°C. Care was taken to maintain the temperature of the nitrogen entering the block at the block temperature in order to minimize thermal gradients within the block chamber. The entire block was wrapped with 19-mm-thick ceramic insulation (Kaowool). A type J Omega iron-constantan thermocouple was inserted into the brass block 10 mm above the ports and was read by an Omega HH-70JC meter (±1°C) to monitor the block temperature. In order to determine the temperature profile within the block, an Omega type T copper-constantan thermocouple was inserted into the chamber and was read by an Omega HH-70TC meter (±1°c). The chamber temperature was determined at the ports, 40 mm above the ports, at the top of the block, and immediately below the cold stage. Typically, temperatures within the chamber were within two to three degrees of the temperature at the ports and the temperature of the block itself. The temperature of the ambient on the chamber axis immediately below the cold stage was generally 5–20°C below the average chamber temperature.

The flow of heated nitrogen entering the block from the bottom served two important purposes. First, it prevented the influx of air into the block, which, as shown in Fig. 2, could interfere with the accurate determination of the droplet temperature by differential quenching of the fluorescence. Second, the nitrogen flow reduced the accumulation of decane vapors in the chamber.

After falling 100 mm, a droplet was intercepted by a laser beam focused to an area approximately 4 mm × 6 mm. A delay between the droplet generator firing and triggering of the laser (or strobe) of 160–200 ms was necessary, depending upon the nitrogen flow rate. Fluorescence emission at right angles to the incident laser light was focused with a 50-mm-dia, 100-mm focal length quartz lens onto the 500 μm entrance slit of the spectrometer. Three 350 nm high-pass filters (total $OD_{337} = 4.1$) were positioned in front of the spectrometer entrance slit to suppress the scattered light at 337 nm. The spectrometer was set so that fluorescence from 200–600 nm fell on the intensified portion of the diode array detector.

Droplet emission spectra were digitized by the OMA system and were stored on disk for later analysis. Background light taken without droplets in the chamber was recorded before each experiment and was subtracted from each droplet emission spectrum. Wavelength calibration of the spectrometer was performed with a low-pressure Hg vapor pencil lamp (Hammamatsu Model C-940-001).

The intensities I_E and I_M were determined as integrals over portions of the spectra using the drop-line integration method (see Fig. 1). The vertical line is the declared boundary between the excimer and monomer emissions. The drop-line wavelength chosen for this study was 408 nm. I_M is the integral of the spectrum from 360 to 408 nm, and I_E is the integral from 408 to 600 nm.

In order to account for any possible heating of the droplets by the laser light, droplet emission spectra were recorded at several power levels. The laser beam was attenuated with chemical filters prepared from solutions of potassium chromate in water. Fluorescence spectra were recorded at laser energies, estimated as the fraction of the attenuated laser pulse energy that was intercepted by the droplet, of approximately 11, 6.4, 3.7, and 1.3 μJ per pulse. The quantity $\ln [I_E/I_M]$ was plotted versus laser power and was extrapolated to zero laser power in order to remove any effect of heating of the droplets by the laser. The extrapolated values of $\ln[I_E/I_M]$ were determined from a least-squares fit of a straight line to the data. The least-squares program also estimates the standard deviation of the intercept, i.e., the error in the extrapolated value of $\ln[I_E/I_M]$. No laser heating effect on the droplets was found at chamber temperatures higher than 80°C; it was a minor effect at lower chamber temperatures.

A calibration curve for the excimer fluorescence thermometer was constructed from emission spectra taken at known temperatures with the same 5.00-mM pyrene solution and identical optical collection system. A calibration sample cell was constructed from 5-mm Pyrex glass tubing pulled to 1 mm at its narrow section, which was then flame-sealed. Approximately 0.5 mL of the solution was placed in the tubing and was then connected to a vacuum line and degassed with three freeze-pump-thaw cycles. The solution was then flame-sealed at its upper end under vacuum. A second tube, to be used as a background reference for the calibration sample, was drawn from the same Pyrex tubing, filled with 0.5 mL of pure decane, and processed in the same manner. The calibration tube was positioned within the chamber with the narrow section centered

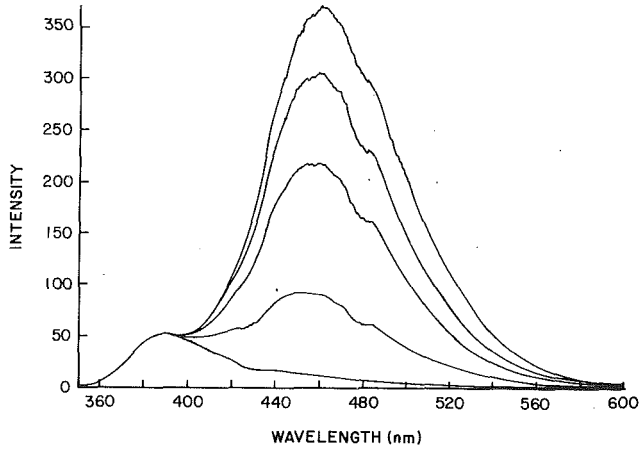

Fig. 5 Fluorescence spectra obtained from 5-mM pyrene in decane calibration sample, excitation wavelength 337 nm. Temperatures, from the top down, are 23, 37, 47, 70-, and 124°C, respectively.

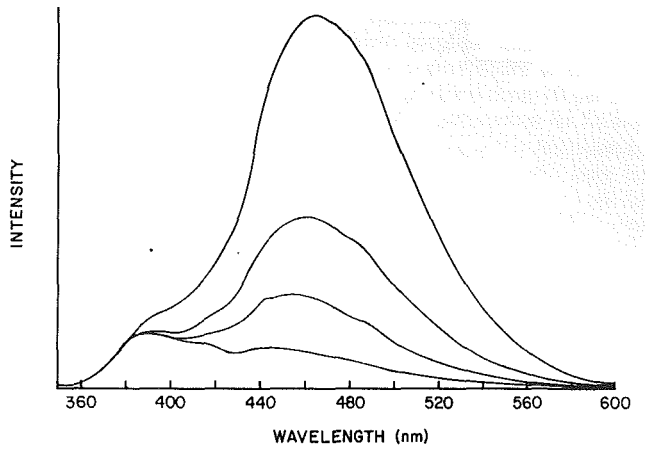

Fig. 7 Fluorescence spectra obtained from 5-mM pyrene in decane droplets, excitation wavelength 337 nm, at chamber temperatures (from top down) of 23, 85, 109, and 257°C

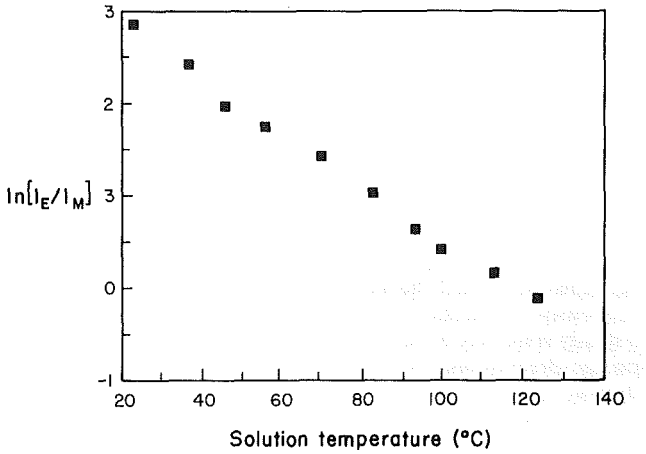

Fig. 6 Calibration curve obtained from data shown in Fig. 5

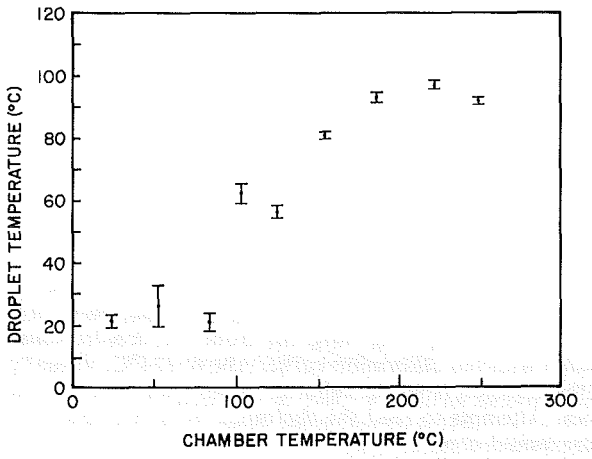

Fig. 8 Droplet temperature as a function of chamber temperature

in the chamber at the port. Due to the large amount of fluorescence available from the calibration sample, it was necessary to attenuate the laser beam with a potassium chromate chemical filter followed by a 1 mm pinhole. Thus, the maximum laser energy falling on the calibration tube was approximately 0.8 μJ per pulse, and no dependence of $\ln[I_E/I_M]$ on laser power was observed for the calibration sample. The calibration sample spectra were corrected for background by subtracting the spectrum obtained with the decane reference sample; no fluorescence was detected from the reference sample. The calibration sample was allowed to equilibrate for 20–30 minutes after the chamber had reached a stable temperature before the spectra at that temperature were collected.

The total emission from the solution decreases approximately a factor of ten as the solution temperature increases from 23°C to 125°C. This does not affect the temperature measurements since the thermometer calibration depends on the ratio I_E/I_M, not the absolute intensities. As long as there is sufficient emitted light available to measure the ratio I_E/I_M accurately, the spectra will yield the temperature of the system accurately.

The droplets were photographed immediately below the cold stage and at the optical access port, with a Ricoh Model KR-30 35 mm SLR camera attached to the eyepiece of a Bausch and Lomb StereoZoom 7 stereomicroscope, which was fitted with a reticle. Droplets were backlighted for photographic measurements via a modified Alpha-M Model 161 stroboscope triggered externally by the pulse, which was otherwise used to trigger the laser. Kodak T-Max 400 Professional B/W film was used to record the negative image of the droplets and was processed in a spiral reel tank with Acufine developer for 13.5 to 14 minutes at 20°C. The processed negatives were cut and mounted as 2×2 in. slides and projected onto a screen for droplet diameter measurements. Absolute sizes were determined by comparison with the photographed reticle. The photographic method has a limit of resolution of droplet diameter of ±5 μm, which corresponds to a volume change of approximately ±7 percent.

Typical vertical instability in the droplet's position at laser interception varied between 0.5 and 5 droplet diameters, depending upon the nitrogen flow rate in the chamber. No lateral instability in the droplet's position occurred at lower temperatures, although at the higher chamber temperatures both vertical and lateral instability resulted, possibly due to turbulence within the chamber. The average velocity of droplets falling through the chamber was 0.6 m/s, resulting in Reynolds numbers for the droplets based on their diameters of between 8.8 at 20°C and 0.3 at 250°C, calculated using the method of Chigier (1981). Every effort was made to maintain the nitrogen flow through the block at a constant rate, but in order to maintain droplet stability, it was occasionally necessary to adjust the flow rate, especially at the higher chamber temperatures.

The spectra in Fig. 2 were taken under front face excitation on a Spex Fluorolog Model DM1B fluorometer. The transmission of the filters was measured with a Hewlett-Packard Model 8450 UV-Vis Spectrophotometer.

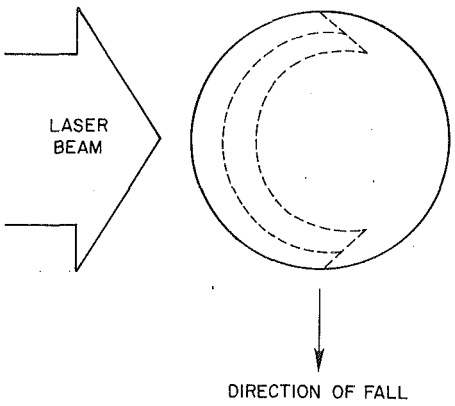

Fig. 9 Penetration of incident laser beam into 225-μm-dia droplet of 5-mM pyrene in decane, excitation wavelength 337 nm. Outer dashed line is the locus of 32 percent transmission ($OD_{337} = 0.5$); inner dashed line is the locus of 10 percent transmission ($OD_{337} = 1.0$).

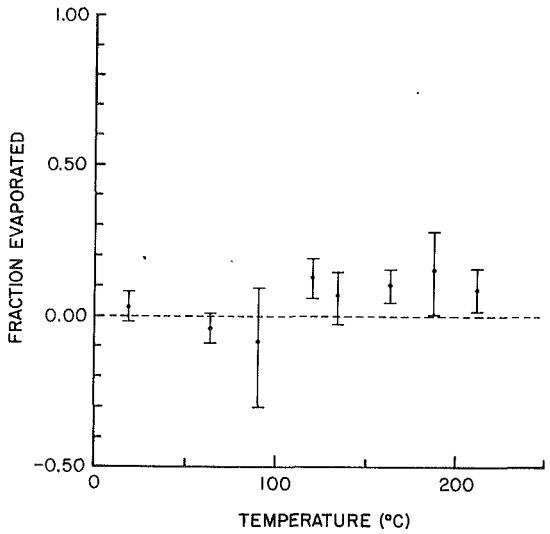

Fig. 10 Fraction of 5 mM pyrene in decane droplet evaporated as a function of chamber temperature. Initial droplet diameter is 225 μm.

IV Results and Discussion

(A) Temperature Calibration. A series of pyrene emission spectra from the calibration sample were collected at temperatures ranging from 23 to 124°C. A stacked plot of selected spectra, normalized to the maximum of the monomer emission, is shown in Fig. 5. A calibration curve was constructed from a plot of $\ln[I_E/I_M]$ versus solution temperature and is shown in Fig. 6. The apparent linearity of the calibration curve is fortuitous, as there is no theoretical reason to expect linearity. The uncertainty in the value of each point was too small to be indicated on the plot, which indicates the reproducibility of the calibration sample data. Droplet temperatures are determined by comparing $\ln[I_E/I_M]$ from the droplet emission spectra with the calibration curve. Above 124°C, virtually all of the emission from the calibration sample is from the monomer. Attempts to read the thermometer above this temperature would contain large errors since the magnitude of the noise in the spectrum approaches the magnitude of the residual emission from the excimer.

(B) Droplet Measurements

1 Temperature Measurements. Figure 7 shows a stacked plot of normalized emission from droplets of the 5.00-mM pyrene in decane solution. The temperature of the decane droplets as a function of chamber temperature is shown in Fig. 8. Since the droplet temperatures were extrapolated to zero laser power, these temperatures represent solely the effect of the heated ambient on the droplet. The uncertainties in each point, indicated by the error bars, were calculated in the two-step process: (1) The measured values of $\ln[I_E/I_M]$ as a function of laser power were fit to a straight line with a linear least-squares program, which also provided a statistical estimate of the uncertainty in $\ln[I_E/I_M]_o$, the value of $\ln [I_E/I_M]$ at the intercept, i.e., with no laser heating, and (2) this estimated uncertainty in $\ln[I_E/I_M]_o$ was used in conjunction with the calibration curve, Fig. 6, to estimate uncertainties in the derived values of the temperature. It is supposed that the error bars obtained with droplets are larger than those obtained with the calibration solutions because of the spatial instability of the droplets, since a comparable number of counts were collected for the droplet and calibration spectra.

The temperatures of the decane droplets increase approximately linearly with an average slope of 0.4°C per degree increase in the chamber temperature up to 200°C. To determine whether the two points at the highest temperatures represent a droplet temperature plateau or simply deviation about the relatively linear temperature trend, more points would be necessary above 250°C; however, severe instability in the position of the droplets prevented collection of either spectral or photographic data above this temperature. There are two reasonable explanations for the decrease in the relatively linear droplet temperature trends. First, evaporation of decane from the droplets may occur at the higher chamber temperatures; thus, pyrene would be concentrated at the droplet surface. The higher concentration of pyrene would shift the monometer–excimer equilibrium toward the excimer, which would result in an erroneously high measured I_E/I_M and a low temperature. Second, a steady state may have been reached in which the heat incident on the droplet results solely in evaporation of liquid at the droplet surface.

It is unlikely that a droplet in a dynamic heat transfer process is at a uniform temperature, and therefore it is necessary to consider how to interpret the temperatures derived from the exciplex fluorescence thermometry experiments. The penetration of the exciting light, and thus the region from which fluorescence is observed, is determined by the optical density of the droplet solution. The molar extinction coefficient of pyrene at 337 nm is approximately 3.6×10^4 M^{-1} cm^{-1} (Berlman, 1971); and thus, for the 5 mM solution used in these droplet experiments, 90 percent (OD = 1) of the light will be absorbed in 56 μm of the solution. A diagram illustrating the penetration of the laser beam into a 225-μm droplet (5 mM pyrene in decane) is shown in Fig. 9. The innermost dotted curve within the droplet represents the locus for absorption of 90 percent (OD = 1) of the incident light; it was constructed by connecting, at 56 μm penetration depth, the light rays refracted into the droplet. The outer dotted line is the locus for penetration to 28 μm, i.e., OD = 0.5; 68 percent of the incident light is absorbed outside of this locus. Note, however, that penetration of the laser light to the full depth occurs only along the axial ray. For off-axis rays, the radial penetration is less because the refracted ray is not along a radius. The actual determination of the radial distribution of the fluorescence reaching the detector is more complicated, since emission from different points within a droplet is refracted into the collecting lens with differing efficiencies. Calculations of the radial distribution of the collected light were made using computer programs, which determine the distribution of absorption within a droplet and the probability of a photon entering a given lens aperture, both within a geometric optics approximation (Melton, 1989). The convolution of these results for a given index of refraction and optical density gives, among other results, the radial distribution of photons entering the lens aperture. Using this program, it was found that for the droplet described

in Fig. 3 and for an f/3.5 lens aperture, 46 percent of the collected light originated from the outer 27 μm of the droplet, and an additional 45 percent originated from the next 27 μm. Thus, 91 percent of the light collected from the droplet originates within the outer 46 μm of the droplet. The temperatures reported are, therefore, averages over the outer 50–60 μm on the irradiated side of the droplet.

The penetration of light into the droplet is dependent on the concentration of the absorber but not on the droplet diameter. If these same techniques were applied to droplets 1 mm in diameter, the temperatures thus determined would result from fluoresence from the outer 10 percent of the droplet radius and thus, would probably be interpretable as surface temperatures.

Within the limitations imposed by the averaging described in the previous paragraph, the reported temperatures are believed to be accurate. In the next section, it is argued that, in this experiment, no more than 10 percent of the droplet mass evaporates, and thus distortions of the temperature measurements due to a changing concentration of pyrene in the surface layers is minimized. Thermal expansion of the droplets is expected as the droplet temperatures increase, but in itself it should have no effect on the derived droplet temperatures since the same effect is present in the calibration sample and is accounted for in the calibration curve.

2 Droplet Evaporation Measurements. Photographs of droplets taken immediately below the cold stage and at the optical access port were compared to determine the fraction of liquid evaporated from the droplets. The fraction evaporated is $f = 1 - (d/d_o')^3$, where d is the droplet diameter at the optical access port and d_o' is the droplet diameter measured at the cold stage and corrected for thermal expansion. The fraction evaporated is shown in Fig. 10 as a function of the ambient temperature. Correction for thermal expansion was made by calculating the volume the initial, cold droplet would have if it were simply raised to the measured droplet temperature, with no evaporation, using the thermal expansion coefficient for decane (Riddick and Bunger, 1970). The diameter of that heated, nonevaporating droplet is d_o'. The correction is necessary since, in this experiment, the changes in droplet diameter due to evaporation and thermal expansion are comparable. Using this method, it is estimated that less than 10 percent of the droplet's volume evaporated at the highest chamber temperatures.

3 Future Work. The results presented here demonstrate that temperature measurements can be made on freely falling droplets and lay the groundwork for continuing experiments to determine the surface temperature of fuel droplets exposed to hot, convective environments. Exciplex fluorescence thermometers with higher optical densities (i.e., complete absorption of the incident light within a few microns of the surface), greater temperature range, and lessened dependence on concentration are under development. Further experiments are planned to investigate the transient and steady-state behavior of droplets by providing for optical access to the droplet throughout its trajectory. With the new thermometry systems, exposures to much hotter environments is planned in order to determine the effects of evaporation on the measured droplet temperature.

V Conclusions

The temperature of droplets of decane exposed to a hot, relatively quiescent, oxygen-free environment have been measured using laser-induced exciplex fluorescence thermometry. The measured droplet temperatures increase approximately 0.4°C per °C increase in the ambient temperature as the ambient temperature is increased to 200°C. Less than 10 percent of the droplet's mass was lost due to evaporation in falling 100 mm at a chamber temperatures of 250°C. The decrease in the droplet heating rate at the highest temperatures may be due to concentration of pyrene at the droplet surface due to evaporation or to attainment of a steady-state temperature for the droplets.

Acknowledgments

Funding for this work was provided by the Army Research Office through contract number DAAL03-87-K-0120. We thank W. A. Sirignano for useful comments.

References

Abdul-Rahman, Y. A. K., 1969, "Drying of Drops Containing Dissolved and Dispersed Gases," M.S. Thesis, University of Wisconsin, Madison, WI.

Abramzon, B., and Sirignano, W. A., 1988, "Droplet Vaporization Model for Spray Combustion Calculations," presented at the AIAA 26th Aerospace Sciences Meeting, Reno, NV, Jan. 11–14, Paper No. AIAA-88-0636.

Aggarwal, S. K., Tong, A. Y., and Sirignano, W. A., 1984, "A Comparison of Vaporization Models in Spray Calculations," *AIAA Journal*, Vol. 22, p. 1448.

Berlman, I. B., 1971, *Handbook of Fluorescence Spectra of Aromatic Molecules*, Academic Press, New York, p. 383.

Birks, J. B., 1970, *Photophysics of Aromatic Molecules*, Wiley-Interscience, New York.

Charlesworth, D. H., and Marshall, W. R., 1959, "Evaporation From Drops Containing Dissolved Solids," *AIChE J.*, Vol. 6, p. 9.

Chigier, N., 1981, *Energy, Combustion and Environment*, McGraw-Hill, New York, p. 273.

Dwyer, H. A., and Sanders, B. R., 1986, "A Detailed Study of Burning Fuel Droplets," *21st Symposium (Int.) on Combustion*, Combustion Institute, Pittsburgh, PA, pp. 633–639.

Faeth, G. M., 1983, "Evaporation and Combustion of Sprays," *Prog. Energy Comb. Sci.*, Vol. 9, p. 1.

Forster, T., 1969, *Excimers*, Angew. Chem. Internat. Editions, Vol. 8, p. 333.

Gogos, G., and Ayyaswamy, P. S., 1988, "A Model for the Evaporation of a Slowly Moving Droplet," *Comb. Flame*, Vol. 74, p. 111.

Gossage, H. E., and Melton, L. A., 1987, "Fluorescence Thermometers Using Intermolecular Exciplexes," *Appl. Optics*, Vol. 26, p. 2256.

Hofmeister, W. H., Bayuzick, R. J., and Robinson, M. B., 1989, "Noncontact Temperature Measurement of a Falling Drop," *Int. J. Thermophys.*, Vol. 10, p. 279.

Law, C. K., 1982, "Recent Advances in Droplet Vaporization and Combustion," *Prog. Energy Comb. Sci.*, Vol. 8, p. 171.

Law, C. K., and Sirignano, W. A., 1977, "Unsteady Droplet Combustion With Droplet Heating—II: Conduction Limit," *Comb. Flame*, Vol. 28, p. 175.

Melton, L. A., 1989, "Efficiency of Capture of Fluorescence From Droplets," unpublished results, University of Texas at Dallas, Richardson, TX.

Melton, L. A., Murray, A. M., and Verdieck, J. F., 1986, "Laser Fluorescence Measurements for Fuel Sprays," *Soc. Photo Opt. Instr. Eng.*, Vol. 644, p. 40.

Murray, A. M., and Melton, L. A., 1985, "Fluorescence Methods for Determination of Temperature in Fuel Sprays," *Appl. Optics*, Vol. 24, p. 2783.

Prakash, S., and Sirignano, W. A., 1978, "Liquid Fuel Droplet Heating With Internal Circulation," *Int. J. Heat Mass Transfer*, Vol. 21, p. 885.

Puri, I. K., and Libby, P. A., 1988, "Droplet Behavior in a Counterflowing Flame," Western States Section/The Combustion Institute 1988 Spring Meeting, Salt Lake City, UT, Mar. 21–22, Paper No. 88–42.

Riddick, J. A., and Bunger, W. B., 1970, *Techniques of Chemistry*, Vol. II, Wiley Interscience, New York, p. 103.

Shield, T. W., Bogy, D. B., and Talke, F. E., 1987, "Drop Formation by DOD Ink-Jet Nozzles: A Comparison of Experiment and Numerical Simulation," *IBM J. Res. Develop.* Vol. 31, p. 96.

Sirignano, W. A., 1983, "Fuel Droplet Vaporization and Spray Combustion Theory," *Prog. Energy Comb. Sci.*, Vol. 9, p. 291.

Sirignano, W. A., 1988, "An Integrated Approach to Spray Combustion Model Development," *Comb. Sci. Tech.*, Vol. 58, p. 231.

Stufflebeam, J. H., 1989, "Exciplex Fluorescence Thermometry of Liquid Fuel," *Appl. Spectrosc.*, Vol. 43, p. 274.

Trommelen, A. M., and Crosby, E. J., 1970, "Evaporation and Drying of Drops in Superheated Vapors," *AIChE J.*, Vol. 16, p. 857.